Available online at www.sciencedirect.com
SCIENCE DIRECT
Journal of Catalysis 233 (2005) 81–89
JOURNAL OF CATALYSIS
www.elsevier.com/locate/jcat

# Oxidation of adamantane with 1 atm molecular oxygen by vanadium-substituted polyoxometalates

Satoshi Shinachi, Mitsunori Matsushita, Kazuya Yamaguchi, Noritaka Mizuno *

*Department of Applied Chemistry, School of Engineering, The University of Tokyo, 7-3-1 Hongo, Bunkyo-ku, Tokyo 113-8656, Japan*

Received 24 February 2005; revised 5 April 2005; accepted 11 April 2005

Available online 23 May 2005

**Abstract**

The oxidation of adamantane with molecular oxygen as a sole oxidant was efficiently promoted by catalyst precursors of vanadium-substituted Keggin-type phosphomolybdates such as $H_4PVMo_{11}O_{40}$, $H_5PV_2Mo_{10}O_{40}$, and $H_6PV_3Mo_9O_{40}$ in butyronitrile. The major product was a tertiary C–H bond oxygenated product of 1-adamantanol, and secondary C–H bond oxygenated products were also formed. The total yield of oxygenated products for the oxidation of adamantane in the presence of $H_5PV_2Mo_{10}O_{40}$ reached 84%. NMR and IR data show that the vanadium-substituted phosphomolybdates, such as $H_4PVMo_{11}O_{40}$ and $H_5PV_2Mo_{10}O_{40}$, decompose to form the monomeric vanadium species ($V^VO_2{}^+$ (main) and $V^{IV}O^{2+}$) and $PMo_{12}O_{40}{}^{3-}$ Keggin anion. The reaction mechanism involving a radical species was proposed from ESR and kinetic data. The catalysts initially abstract the hydrogen of adamantane to form the adamantyl radical and reduced catalysts. This step would be promoted mainly by the vanadium species, such as $V^VO_2{}^+$, and the phosphomolybdates, $PMo_{12}O_{40}{}^{n-}$, enhance the activity. The adamantyl radical formed promotes the successive formation of the key intermediates, such as adamantyl radical and hydroperoxide species.


*Keywords:* Adamantane; Molecular oxygen; Oxidation; Polyoxometalate; Vanadium

## 1. Introduction

The development of efficient methods for the oxidation of unactivated C–H bonds of alkanes with molecular oxygen is of great importance from industrial and synthesis standpoints [1–3]. Recently, much attention has been paid to the oxidation of adamantane because the substituted-adamantane derivatives, especially mono- or di-substituted ones, can be used as important precursors for photoresists and medicines [4–6]. Although many polysubstituted adamantanes have been easily synthesized, the synthesis of mono- or di-oxygenated ones is very difficult [7]. Typically, tertiary mono- and di-oxygenated adamantanes, such as 1-adamantanol and 1,3-adamantanediol, are synthesized by the bromination of adamantane with the use of molecular bromine, followed the hydrolysis of the corresponding brominated ones. Secondary mono-oxygenated adamantanes such as 2-adamantanol are synthesized by the rearrangement of tertiary hydroxylated adamantanes with the use of concentrated $H_2SO_4$ [8–10]. From the standpoint of green chemistry, these conventional methods are undesirable because they need multistep reactions and hazardous reagents to produce large quantities of by-products [8–10]. Adamantane has four relatively weak tertiary C–H bonds, and the autooxidation may take place via a radical-chain mechanism at elevated temperatures. However, even in the case of adamantane, it is known that such autooxidation cannot be efficiently catalyzed by simple transition-metal salts such as $Co(acac)_2$, $Mn(OAc)_2$, and $Mn(acac)_3$ under mild reaction conditions (below 373 K) [11,12]. In these contexts, there is a great demand for the development of one-step catalytic adamantane oxidation systems with an environmentally friendly oxidant of molecular oxygen without

* Corresponding author. Fax: +81 3 5841 7220.
*E-mail address:* tmizuno@mail.ecc.u-tokyo.ac.jp (N. Mizuno).

0021-9517/$ – see front matter 
doi:10.1016/j.jcat.2005.04.012

hazardous reagents which can reduce environmentally undesirable wastes.

Although there have been several reports on the liquid-phase oxidation of adamantane with molecular oxygen, these systems need reductants such as hydroquinone [13], metals of zinc [14–16] and iron [17], and aldehydes [18–21]. Ishii and co-workers have developed an efficient alkane oxidation system with a combined catalyst of *N*-hydroxyphthalimide (NHPI) and $Co(acac)_2$ [11,12], and the NHPI almost decomposed to phthalic acid and the other compounds (used by our group). Therefore, a large amount of NHPI (at least 10 mol%) was required to achieve the high yields of the corresponding oxygenated products, and the catalyst could not be recycled. Thus, there are only limited examples of the oxidation of adamantane with molecular oxygen under mild reaction conditions with only a small amount of transition-metal catalysts [22–25].

Polyoxometalates catalyze the transformation of various kinds of functional groups because the redox and acid properties can be controlled at the atomic or molecular level through a change of the constituent elements [26–31]. Therefore, the catalytic function of polyoxometalates has attracted much attention. Various kinds of polyoxometalate-catalyzed liquid-phase oxidation reactions have been reported [32–44], and Keggin-type phosphovanadomolybdates such as $H_4PVMo_{11}O_{40}$, $H_5PV_2Mo_{10}O_{40}$, and $H_6PV_3Mo_9O_{40}$ have been reported to be catalytically active for the reactions [45–49]. However, to our knowledge, there has been no application of the vanadium-substituted polyoxometalates to the oxidation of adamantane with molecular oxygen as a sole oxidant. In this paper, we report on the oxidation of adamantane with 1 atm of molecular oxygen in butyronitrile without any additives promoted by vanadium-substituted polyoxometalates. Notably, the vanadium-substituted polyoxometalates showed higher catalytic activity than did transition-metal salts such as $Co(OAc)_2$, $Mn(OAc)_2$, and $VO(acac)_2$, which are widely used as catalysts for free radical autooxidations [1–3,11,12]. We also investigated the catalyst state and possible reaction path.

## 2. Experimental

### 2.1. General

GC analyses were performed on a Shimadzu GC-17A with a flame ionization detector equipped with a DB-WAX capillary column (internal diameter 0.25 mm, length 30 m). Mass spectra were recorded on a Shimadzu GCMS-QP2010 at an ionization voltage of 70 eV equipped with a DB-WAX capillary column (internal diameter 0.25 mm, length 30 m). NMR spectra were recorded on a JEOL JNM-EX-270. $^{31}$P NMR spectra of polyoxometalates were measured at 109.24 MHz in butyronitrile. $H_3PO_4$ (85%) was used as an external standard. $^{51}$V NMR spectra of polyoxometalates were measured at 70.75 MHz in butyronitrile. $VOCl_3$ was used as an external standard. IR spectra were measured on a Jasco FT/IR-460 Plus with KBr disks. ESR measurements were made at 100 K (X-band) with a JEOL JES-RE-1X spectrometer. The microwave power, modulation width, and time constant were 1.0 mW, 1.0 mT, and 0.1 s, respectively. A reactor directly connected to an ESR tube was used to avoid exposing the sample to air. After a certain catalytic reaction period, the reaction solution was transferred into the ESR tube, and the tube was sealed by firing. The simulation was carried out with the assumption of axial symmetry for vanadium, according to the literature [50].

Solvents were analytical grade (Tokyo Kasei) and were purified before use [51]. Adamantane and 1,3-dimethyladamantane were commercially obtained from Tokyo Kasei (reagent grade) and purified before use [51].

### 2.2. Catalysts

Phosphometalates (except for $H_3PMo_{12}O_{40}$, $H_4PVMo_{11}O_{40}$, $[V^{IV}O(H_2O)_5]H[PMo_{12}O_{40}]$, and $(NH_4)_5[PV^{IV}Mo_{11}O_{40}]$) were supplied by Nippon Inorganic Colour and Chemical Co., Ltd. and used after recrystallization from water. $H_3PMo_{12}O_{40}$ (Kanto) was used as received. $H_4PVMo_{11}O_{40}$ [52], $[V^{IV}O(H_2O)_5]H[PMo_{12}O_{40}]$ [53], and $(NH_4)_5[PV^{IV}Mo_{11}O_{40}]$ [54] were synthesized with procedures described in the literature.

#### 2.2.1. $H_4PVMo_{11}O_{40}$

Disodium hydrogen phosphate (12.5 mmol) was dissolved in 25 ml of water and mixed with sodium metavanadate (12.5 mmol) that had been dissolved in 25 ml of boiling water. The mixture was cooled and acidified with 1.3 ml of concentrated sulfuric acid. To this mixture was added an aqueous solution (50 ml) of sodium molybdate dihydrate (138 mmol). Finally, 21 ml of concentrated sulfuric acid was slowly added with vigorous stirring, which was followed by a color change from dark red to light red. The heteropoly acid was then extracted with 100 ml of diethyl ether. In this extraction, the heteropoly etherate was present in the middle layer. After the separation, a stream of air was passed through the heteropoly etherate layer to free it of ether. The orange solid obtained was dissolved in 13 ml of water and concentrated in a vacuum desiccator until the crystals appeared. The orange crystals were filtered, washed with water, and dried under vacuum (23% yield). Anal. calcd. for $H_4PVMo_{11}O_{40}\cdot 17H_2O$: P, 1.48; V, 2.44; Mo, 50.56. Found: P, 1.61; V, 2.89; Mo, 49.82. IR (KBr) ($cm^{-1}$): 1078 (sh, $\nu_{as}$(P–$O_a$–V)), 1061 (s, $\nu_{as}$(P–$O_a$)), 960 (s, $\nu_{as}$(Mo–$O_d$)), 866 (s, $\nu_{as}$(Mo–$O_b$–M)) (M = Mo, V), 786 (s, $\nu_{as}$(Mo–$O_c$–M)) ($O_a$, inner oxygen; $O_b$, corner-shared oxygen; $O_c$, edge-shared oxygen; $O_d$, terminal oxygen). $^{31}$P NMR (butyronitrile, 109.24 MHz, 0.67 mM): −2.06 ppm (the purity by $^{31}$P NMR $\geqslant$ 80%). UV–vis (acetonitrile, 109.24 MHz, 0.02 mM): $\lambda_{max}$ 308 nm ($\varepsilon = 2.22\times10^5$ $cm^{-1}\,M^{-1}$).

#### 2.2.2. $[V^{IV}O(H_2O)_5]H[PMo_{12}O_{40}]$

$H_3PMo_{12}O_{40}$ (4.85 mmol) was dissolved in 10 ml of water. Barium hydroxide octahydrate (4.85 mmol) was added to the solution in small portions to keep the pH constant (pH 0.75). Vanadyl sulfate pentahydrate (4.85 mmol) was then quickly added, and the solution was kept at room temperature for 0.5 h. The barium sulfate precipitate was filtered off, and then the resultant solution was kept at 277 K to yield green crystals (27% yield). Anal. calcd for $[VO(H_2O)_5]H[PMo_{12}O_{40}] \cdot 8H_2O$: P, 1.46; V, 2.40; Mo, 54.18. Found: P, 1.71; V, 2.36; Mo, 54.15. IR (KBr) ($cm^{-1}$): 1065 (s, $\nu_{as}$(P–$O_a$)), 962 (s, $\nu_{as}$(Mo–$O_d$)), 870 (s, $\nu_{as}$(Mo–$O_b$–M)) (M = Mo, V), 790 (s, $\nu_{as}$(Mo–$O_c$–M)). $^{31}$P NMR (butyronitrile, 109.24 MHz, 0.67 mM): −2.50 ppm. UV–vis (acetonitrile, 0.02 mM): $\lambda_{max}$ 308 nm ($\varepsilon = 2.19 \times 10^5\ cm^{-1}\,M^{-1}$).

#### 2.2.3. $(NH_4)_5[PV^{IV}Mo_{11}O_{40}]$

Ammonium heptamolybdate (7.8 mmol) was dissolved in 51 ml of hot water. The solution was cooled to room temperature, followed by acidification with 1.5 ml of glacial acetic acid. We prepared the second solution by dissolving vanadium oxide sulfate pentahydrate (5 mmol) in 15 ml of water containing 0.41 ml of phosphoric acid (75% by volume). The two solutions were cooled to 277 K, and then a solution of vanadyl sulfate was added to that of molybdate. After 0.5 h, the dark blue solution was filtered, and ammonium nitrate (56.3 mmol) was added to the filtrate, which was followed by the formation of a dark blue crystalline solid. The solid was filtered and washed with cold water to eliminate a trace of ammonium nitrate (28% yield). Anal. calcd. for $(NH_4)_5[PV^{IV}Mo_{11}O_{40}] \cdot H_2O$: H, 1.87; N, 3.45; P, 1.53; V, 2.51; Mo, 52.00. Found: H, 2.02; N, 3.54; P, 1.71; V, 2.73; Mo, 49.24. IR (KBr) ($cm^{-1}$): 1066 (sh, $\nu_{as}$(P–$O_a$–V)), 1051 (s, $\nu_{as}$(P–$O_a$)), 945 (s, $\nu_{as}$(Mo–$O_d$)), 865 (s, $\nu_{as}$(Mo–$O_b$–M)) (M = Mo, V), 777 (s, $\nu_{as}$(Mo–$O_c$–M)). UV–vis (acetonitrile, 0.02 mM): $\lambda_{max}$ 672 nm ($\varepsilon = 8.55 \times 10^3\ cm^{-1}\,M^{-1}$), 308 nm ($\varepsilon = 2.22 \times 10^5\ cm^{-1}\,M^{-1}$).

### 2.3. Procedure for oxidation of adamantane and 1,3-dimethyladamantane

Oxidation of adamantane (or 1,3-dimethyladamantane) was carried out in a glass vial containing a magnetic stir bar. A typical procedure for the adamantane oxidation was as follows. Into a glass vial were successively placed adamantane (1 mmol), catalyst (2 μmol), and butyronitrile (3 ml). Then 1 atm of molecular oxygen was introduced into the system. The reaction mixture was heated at 356 K. The yields were determined by GC analyses with naphthalene as an internal standard. All of the products were confirmed by GC analysis in combination with mass spectroscopy.

### 2.4. Kinetic study

Oxidation of adamantane was performed with the same procedure as described above. The reaction conditions are given in the figure captions. Reaction rates ($R_0$) for the kinetic analyses were determined from the slope of reaction profiles (conversion vs. time plots) at low conversion (< 10%) of the substrate after the induction period.

## 3. Results and discussion

### 3.1. Oxidation of adamantane

First, the oxidation of adamantane was carried out with $H_5PV_2Mo_{10}O_{40}$ at 356 K under 1 atm of molecular oxygen in various solvents. The results are summarized in Table 1. The oxidation did not proceed in the absence of

Table 1
Oxidation of adamantane with molecular oxygen in various solvents[a]

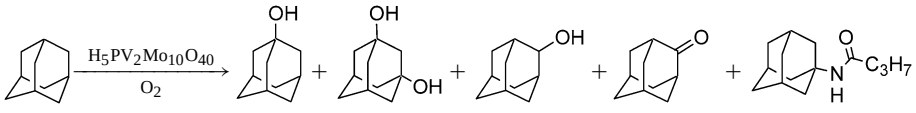


**1** **2** **3** **4** **5**

| Entry | Solvent | Yield (%) | Selectivity (%) | | | | |
|---|---|---|---|---|---|---|---|
| | | | **1** | **2** | **3** | **4** | **5** |
| 1 | Butyronitrile | 46 | 54 | 17 | 14 | 16 | 19 |
| 2[b] | Butyronitrile | 84 | 43 | 24 | 11 | 20 | 12 |
| 3 | Diethylketone | 30 | 65 | 11 | 17 | 17 | – |
| 4 | Cyclopentanone | 22 | 68 | 14 | 12 | 16 | – |
| 5 | Dimethylformamide | 12 | 80 | – | 19 | 11 | – |
| 6 | Acetic acid | 11 | 65 | – | 15 | 20 | – |
| 7 | Acetonitrile | < 1 | – | – | – | – | – |
| 8 | Toluene | < 1 | – | – | – | – | – |
| 9 | 1,2-Dichloroethane | < 1 | – | – | – | – | – |

[a] Reaction conditions: $H_5PV_2Mo_{10}O_{40}$ (2 μmol), adamantane (1 mmol), solvent (3 ml), 356 K, 96 h under 1 atm of molecular oxygen. Yields and selectivities were determined by gas chromatographic analysis using naphthalene as an internal standard.

[b] 288 h.

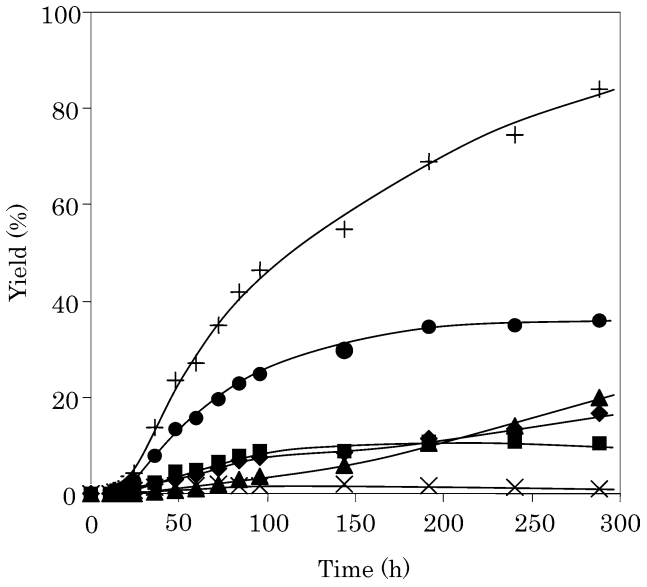


Fig. 1. Reaction profiles of the oxidation of adamantane with molecular oxygen catalyzed by $H_5PV_2Mo_{10}O_{40}$. Total yield (+), yields of 1-adamantanol (●), 1,3-adamantanediol (▲), 2-adamantanol (×), 2-adamantanone (◆), and *N*-(1-adamantyl)butylamide (■). Reaction conditions: $H_5PV_2Mo_{10}O_{40}$ (2 μmol, 0.67 mM), adamantane (1 mmol), butyronitrile (3 ml), 356 K under 1 atm of molecular oxygen.

$H_5PV_2Mo_{10}O_{40}$ in any solvents. Among the solvents tested, butyronitrile gave the highest yields of the corresponding oxygenated products. 1,2-Dichloroethane, toluene, and acetonitrile, in which adamantane and/or catalyst were not soluble, were poor solvents. Therefore, the oxidation was carried out thereafter in butyronitrile. Fig. 1 shows the reaction profiles for butyronitrile. The oxidation proceeded with an induction period (10–11 h). The major product was tertiary C–H bond oxygenated 1-adamantanol; secondary C–H bond oxygenated products were also formed. After ca. 36 h, the successive oxidation of 1-adamantanol to 1,3-adamantanediol proceeded. In the present oxidation, *N*-(1-adamantyl)butylamide was also produced by the Ritter reaction of 1-adamantanol with butyronitrile. When the reaction time was prolonged to 288 h, the total yield of the products reached 84%. From the standpoint of the product yields, this value is higher than those reported so far for the oxidation of adamantane with molecular oxygen as a sole oxidant under mild conditions (below 373 K): Ru-substituted sandwich-type polyoxometalate[$(n\text{-}C_8H_{17})_3CH_3N]_{11}$ [$WZnRu_2(OH)(H_2O)(ZnW_9O_{34})_2$] (57%) [23], Ru-substituted tungstosilicate [$(n\text{-}C_4H_9)_4N]_4H[SiW_{11}Ru(H_2O)O_{39}$] (42%) [22], Ni and Fe-substituted tungstophosphate [$(n\text{-}C_4H_9)N]_4H_6[PW_9O_{37}\{Fe_2Ni(OAc)_3\}$] (29%) [24], and K[Ru(saloph)$Cl_2$] (13%) [25]. After the oxidation was finished, adamantane was re-added to the reaction solution, and the solution was again heated at 356 K in the presence of molecular oxygen. The oxidation again proceeded without an induction period, and with almost the same rate and product distribution as those observed for the first run, showing that $H_5PV_2Mo_{10}O_{40}$ is intrinsically recyclable.

Table 2 lists the results for the oxidation of adamantane with molecular oxygen in the presence of various catalysts. Among the polyoxometalates tested, vanadium-substituted polyoxometalates were the most effective catalysts, and the yield decreased in the order $H_5PV_2Mo_{10}O_{40} \approx H_6PV_3Mo_9O_{40} \geqslant H_4PVMo_{11}O_{40} > H_4PVW_{11}O_{40} \gg H_3PMo_{12}O_{40} > H_3PW_{12}O_{40}$. The vanadium-substituted polyoxometalates exhibited higher catalytic activity than those of $H_3PMo_{12}O_{40}$ and $H_3PW_{12}O_{40}$, showing that vanadium is an indispensable component for attaining high yields of

Table 2
Oxidation of adamantane with molecular oxygen in the presence of various catalysts[a]

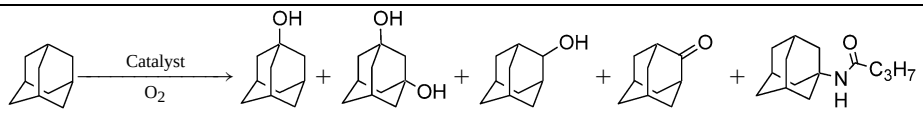


**1** **2** **3** **4** **5**

| Entry | Catalyst | Yield (%) | Selectivity (%) | | | | | $C^3$–H/$C^2$–H[b] |
|---|---|---|---|---|---|---|---|---|
| | | | **1** | **2** | **3** | **4** | **5** | |
| 1 | $H_5PV_2Mo_{10}O_{40}$ | 46 | 54 | 17 | 14 | 16 | 19 | 13.1 |
| 2 | $H_6PV_3Mo_9O_{40}$ | 46 | 54 | 17 | 14 | 16 | 19 | 13.1 |
| 3 | $H_4PVMo_{11}O_{40}$ | 39 | 54 | 16 | 15 | 15 | 20 | 12.9 |
| 4 | $H_4PVW_{11}O_{40}$ | 26 | 62 | 15 | 16 | 15 | 12 | 12.0 |
| 5 | $H_3PMo_{12}O_{40}$ | 7 | 50 | 8 | 8 | 12 | 22 | 13.2 |
| 6 | $H_3PW_{12}O_{40}$ | < 1 | – | – | – | – | – | – |
| 8 | $VO(acac)_2$ | 29 | 78 | – | – | 22 | – | 10.6 |
| 9 | $Co(OAc)_2$ | 17 | 80 | 2 | 7 | 11 | – | 14.0 |
| 10 | $Mn(OAc)_2$ | < 1 | – | – | – | – | – | – |
| 11 | None | < 1 | – | – | – | – | – | – |

[a] Reaction conditions: catalyst (2 μmol), adamantane (1 mmol), butyronitrile (3 ml), 356 K, 96 h under 1 atm of molecular oxygen. Yields and selectivities were determined by gas chromatographic analysis using naphthalene as an internal standard. Carbon balance for each reaction was more than 93%.

[b] The selectivity parameter defined by the relative reactivity of tertiary C–H bonds to secondary C–H bonds ($= \{(\mathbf{1} + \mathbf{2} \times 2 + \mathbf{5})/4\}/\{(\mathbf{3} + \mathbf{4})/12\}$).

oxygenated adamantanes.[1] It was noted that the vanadium-substituted polyoxometalates showed higher catalytic activity than those of transition-metal salts such as $Co(OAc)_2$, $Mn(OAc)_2$, and $VO(acac)_2$, which are widely used as catalysts for free radical autooxidations.

### 3.2. State of the catalyst

We investigated the state of the catalyst with ESR spectroscopy in more detail. In the measurements, 1,3-dimethyladamantane was used as a substrate because the solubility of adamantane in butyronitrile was low (below 298 K) and the added adamantane was partly insoluble. When $H_5PV_2Mo_{10}O_{40}$ was used in the following ESR measurements, the spectrum was very complicated, as shown in Fig. 2a, and could not be well reproduced by the simulation with parameters of one species because $H_5PV_2Mo_{10}O_{40}$ was an inseparable mixture of five isomers, as has been reported [55–57]. Therefore, the following ESR measurements were carried out with $H_4PVMo_{11}O_{40}$. The butyronitrile solution of $H_4PVMo_{11}O_{40}$ (0.67 mM) without 1,3-dimethyladamantane was completely ESR silent, even after treatment at 356 K under argon. Five hundred equivalents of 1,3-dimethyladamantane with respect to $H_4PVMo_{11}O_{40}$ were added to the solution, which was kept at 356 K under 1 atm of argon. After 6 h, the color of the solution had changed from yellow to yellow-green, suggesting the reduction of $H_4PVMo_{11}O_{40}$. When adamantane was used as a substrate, the same color change was observed. The yellow-green color was not the same as that of $(NH_4)_5[PV^{IV}Mo_{11}O_{40}]$ (blue), but the same as that of $[V^{IV}O(H_2O)_5]H[PMo_{12}O_{40}]$ in butyronitrile. Then the ESR spectrum was measured at 100 K (Fig. 2b). The hyperfine structure of vanadium was observed, and the ESR spectrum was well reproduced by simulation with the following parameters: $g_\perp = 1.984$, $g_\parallel = 1.945$, $A_\perp = 6.4$ mT, $A_\parallel = 17.1$ mT (dotted line in Fig. 2b). These parameters are typical of the parallel and perpendicular features of $V^{4+}$ in an axial ligand field [54,58]. The ESR spectra of $[V^{IV}O(H_2O)_5]H[PMo_{12}O_{40}]$ and $(NH_4)_5[PV^{IV}Mo_{11}O_{40}]$ at 100 K are shown in Figs. 2c and d, respectively. The spectra were well reproduced with the following parameters: $[V^{IV}O(H_2O)_5]H[PMo_{12}O_{40}]$ ($g_\perp = 1.982$, $g_\parallel = 1.938$, $A_\perp = 6.7$ mT, $A_\parallel = 17.7$ mT, dotted line in Fig. 2c); $(NH_4)_5[PV^{IV}Mo_{11}O_{40}]$ ($g_\perp = 1.977$, $g_\parallel = 1.939$, $A_\perp = 5.3$ mT, $A_\parallel = 14.8$ mT, dotted line in Fig. 2d).[2] It was found that the parameters of the hyperfine structure of $H_4PVMo_{11}O_{40}$ reduced with 1,3-dimethyladamantane were not similar to those of $(NH_4)_5[PV^{IV}Mo_{11}O_{40}]$, but to those of $[V^{IV}O(H_2O)_5]H[PMo_{12}O_{40}]$. The ESR spectrum of $H_5PV_2Mo_{10}O_{40}$ reduced with 1,3-dimethyladamantane (Fig. 2a) was similar to that of $[V^{IV}O(H_2O)_5]H[PMo_{12}O_{40}]$.

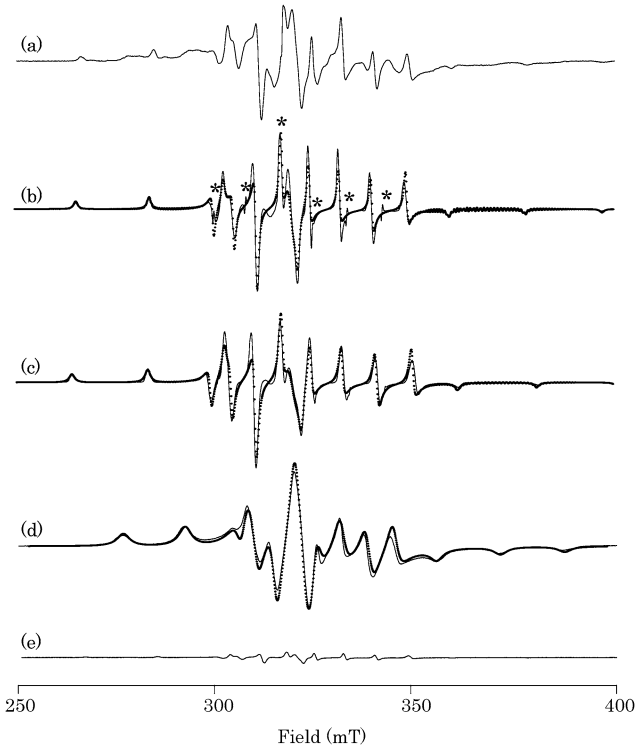


Fig. 2. ESR spectra of vanadium-containing polyoxometalates at 100 K. (a) $H_5PV_2Mo_{10}O_{40}$ (0.67 mM) was treated with 1,3-dimethyladamantane (500 eq) in butyronitrile under 1 atm of argon at 356 K for 6 h. The signal intensity corresponds to the extent of reduction of 0.5 electrons per polyanion. (b) $H_4PVMo_{11}O_{40}$ (0.67 mM) in butyronitrile was treated with 1,3-dimethyladamantane (500 eq) under 1 atm of argon at 356 K for 6 h. The signal intensity corresponds to the extent of reduction of 0.3 electrons per polyanion. (c) $[V^{IV}O(H_2O)_5]H[PMo_{12}O_{40}]$ in butyronitrile. (d) $(NH_4)_5[PV^{IV}Mo_{11}O_{40}]$ in acetonitrile. (e) The above solution (b) was treated with 1 atm of molecular oxygen at 356 K for 10 min. The signal intensity corresponds to the extent of reduction of 0.03 electrons per polyanion. The dotted line in (b)–(d) were obtained by the simulation (see text). Six asterisks in (b) were assigned to the signals of the Mn marker.

$^{31}P$ and $^{51}V$ NMR measurements were carried out with the same sample ($H_4PVMo_{11}O_{40}$ + 1,3-dimethyladamantane + butyronitrile) as that used for the ESR measurements. The fresh $H_4PVMo_{11}O_{40}$ in butyronitrile showed a $^{31}P$ NMR signal at −2.06 ppm (Fig. 3a). The $^{31}P$ NMR spectrum of $H_4PVMo_{11}O_{40}$ obtained after it was used for the oxidation of 1,3-dimethyladamantane showed an intense signal at −2.59 ppm (Fig. 3b). The signal at −2.59 ppm can probably be assigned to $PMo_{12}O_{40}^{3-}$, since the $^{31}P$ NMR

[1] The oxidation of adamantane was carried out with $VO(acac)_2$ under the conditions in Table 2. The yields of 1-adamantanol, 1,3-adamantanediol, 2-adamantanol, and 2-adamantanone were 23, < 1, < 1, and 6%, respectively, and the total yield was lower than those with vanadium-substituted phosphomolybdates. The butyronitrile solution of $VO(acac)_2$ was completely $^{51}V$ NMR silent. The $^{51}V$ NMR spectrum of $VO(acac)_2$ after the oxidation of 1,3-dimethyladamantane under the conditions in Fig. 2 showed a signal at −360 ppm which may be assigned to $V^VO_2^+$ species in the presence of the acetyl acetonato ligand.

[2] The ESR spectrum of $(NH_4)_5[PV^{IV}Mo_{11}O_{40}]$ was measured in acetonitrile because $(NH_4)_5[PV^{IV}Mo_{11}O_{40}]$ was insoluble in butyronitrile. It was confirmed for $[V^{IV}O(H_2O)_5]H[PMo_{12}O_{40}]$ that the parameters of the hyperfine structure of vanadium in acetonitrile was the same as those in butyronitrile.

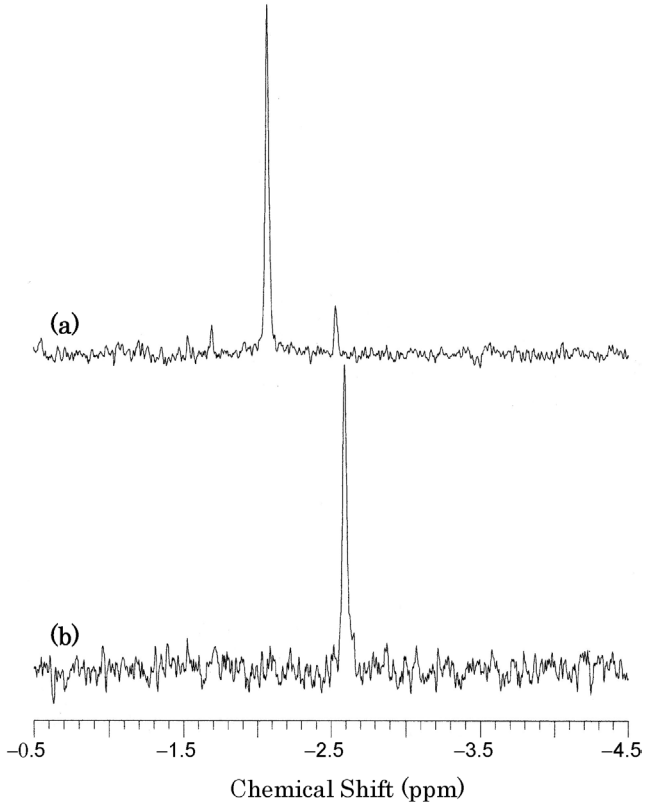


Fig. 3. $^{31}$P NMR spectra of $H_4PVMo_{11}O_{40}$ in butyronitrile before and after the oxidation of 1,3-dimethyladamantane. (a) As-synthesized $H_4PVMo_{11}O_{40}$ (0.67 mM). (b) After the oxidation of 1,3-dimethyladamantane. Reaction conditions: $H_4PVMo_{11}O_{40}$ (2 μmol, 0.67 mM), 1,3-dimethyladamantane (1 mmol), butyronitrile (3 ml), 356 K, 24 h, under 1 atm of molecular oxygen.

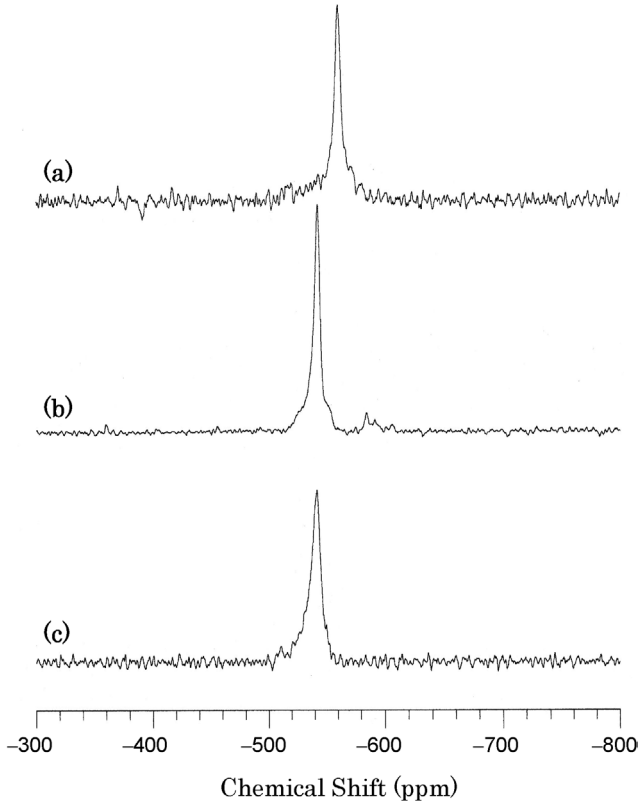


Fig. 4. $^{51}$V NMR spectra of $H_4PVMo_{11}O_{40}$ and $V^VO_2^+$ species in butyronitrile. (a) As-synthesized $H_4PVMo_{11}O_{40}$ (0.67 mM). (b) After the oxidation of 1,3-dimethyladamantane. (c) $V^VO_2^+$ species (0.67 mM). Reaction conditions: $H_4PVMo_{11}O_{40}$ (2 μmol, 0.67 mM), 1,3-dimethyladamantane (1 mmol), butyronitrile (3 ml), 356 K, 24 h, under 1 atm of molecular oxygen.

spectra of $H_3PMo_{12}O_{40}$ and $[V^{IV}O(H_2O)_5]H[PMo_{12}O_{40}]$ in butyronitrile showed signals at −2.54 and −2.50 ppm (see Fig. S1 in the supplementary material), respectively, and the positions were close to −2.59 ppm. The $^{31}$P NMR spectrum of $H_4PVMo_{11}O_{40}$ obtained after it was used for adamantane oxidation was measured by the removal of insoluble adamantane with decantation after the reaction; it also showed an intense signal at −2.63 ppm (see Fig. S2 in the supplementary material). The $^{51}$V NMR spectrum of fresh $H_4PVMo_{11}O_{40}$ in butyronitrile showed a signal at −560 ppm (Fig. 4a). The $^{51}$V NMR spectrum of $H_4PVMo_{11}O_{40}$ obtained after it was used for the oxidation of 1,3-dimethyladamantane showed a signal at −542 ppm (Fig. 4b). The signal at −542 ppm was assigned to $V^VO_2^+$ species, since the chemical shift was almost the same as that of $V^VO_2^+$ species in butyronitrile (−541 ppm, Fig. 4c) prepared with methods described in the literature [59]. The $^{51}$V NMR spectrum of $H_4PVMo_{11}O_{40}$ obtained after it was used for adamantane oxidation was measured in the same way as that for the $^{31}$P NMR spectrum measurement and showed a signal at −541 ppm (see Fig. S3 in the supplementary material).

The IR spectrum of fresh $H_4PVMo_{11}O_{40}$ showed bands characteristic of the Keggin structure: 1078 (sh, $\nu_{as}$(P–$O_a$–V)), 1061 (s, $\nu_{as}$(P–$O_a$)), 960 (s, $\nu_{as}$(Mo–$O_d$)), 866 (s, $\nu_{as}$(Mo–$O_b$–M)) (M = Mo, V), and 786 $cm^{-1}$ (s, $\nu_{as}$(Mo–$O_c$–M)). After the adamantane oxidation, the band position and intensities of the recovered catalyst were almost unchanged, except that the shoulder $\nu_{as}$(P–$O_a$–V) band intensity was much decreased.

These ESR, NMR, and IR data show the elimination of the vanadium from the Keggin anion framework to form monomeric $V^VO_2^+$ species and $PMo_{12}O_{40}^{3-}$ Keggin anions during the oxidation, which are likely catalytically active for the present adamantane oxidation.

After $H_4PVMo_{11}O_{40}$ was reduced with 1,3-dimethyladamantane in butyronitrile, 1 atm of molecular oxygen was introduced to the solution, resulting in a quick change (within 10 min) of the color from yellow-green to yellow and the near disappearance of ESR signals (Fig. 2e). These facts indicate that the reduced catalyst is easily reoxidized by molecular oxygen.

### 3.3. Reaction mechanism

As mentioned, the oxidation of adamantane proceeded with an induction period (10–11 h). When a free radical inhibitor of 2,6-di-*tert*-butyl-*p*-cresol was added to the re-

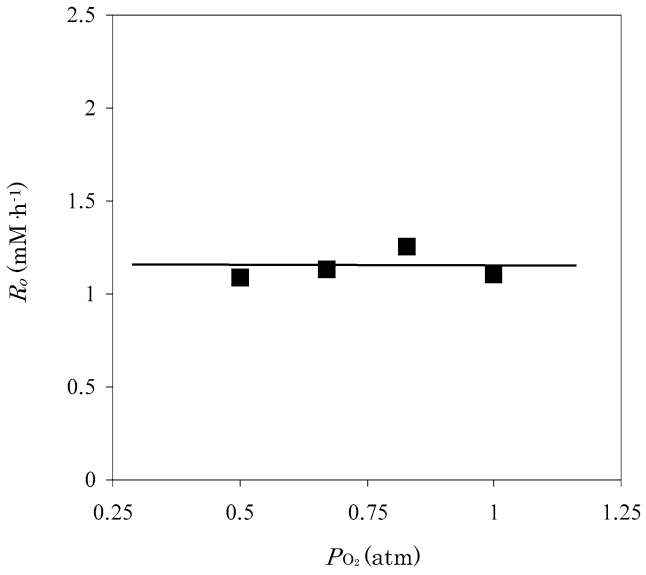


Fig. 5. Dependence of reaction rate ($R_0$) on the partial pressure of molecular oxygen ($p_{O_2}$). Reaction conditions: $H_5PV_2Mo_{10}O_{40}$ (2 μmol), adamantane (1 mmol), butyronitrile (3 ml), 356 K. $p_{O_2} = 0.5$–1.0 atm. $R_0$ values were determined from the reaction profiles (conversion *vs.* time curves) at low conversion (< 10%) of adamantane.

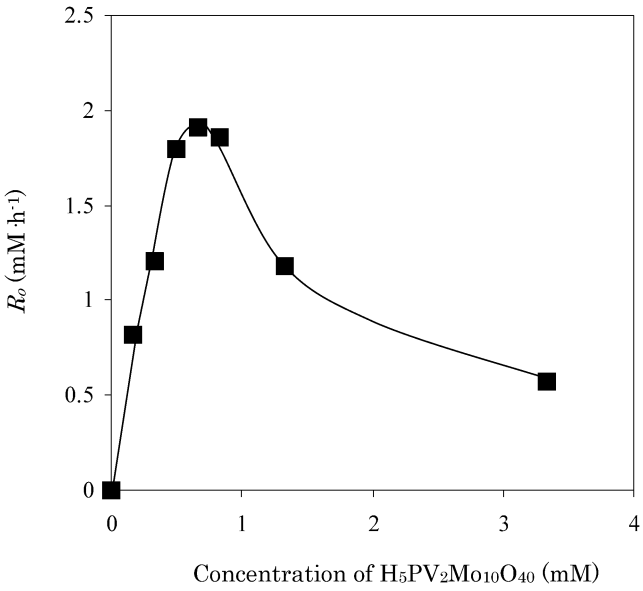


Fig. 6. Dependence of reaction rate ($R_0$) on concentration of $H_5PV_2Mo_{10}O_{40}$. Reaction conditions: $H_5PV_2Mo_{10}O_{40}$ (~ 3.33 mM), adamantane (1 mmol), butyronitrile (3 ml), 356 K, 96 h under 1 atm of molecular oxygen. $R_0$ values were determined from the reaction profiles (conversion *vs.* time curves) at low conversion (< 10%) of adamantane.

action solution, the oxidation of adamantane was immediately stopped. When a radical initiator ($\alpha,\alpha'$-azobisisobutyronitrile (AIBN) or *tert*-butylhydroperoxide (TBHP)) was added to the reaction solution in the presence of $H_5PV_2Mo_{10}O_{40}$, the induction period almost disappeared (see Fig. S5 in the supplementary material). The reaction rate obtained by the slope of the linear line after the induction period was independent of the pressure of the molecular oxygen, as shown in Fig. 5 ($p_{O_2} \geqslant 0.5$ atm). The reaction rate increased with the increase in concentration of $H_5PV_2Mo_{10}O_{40}$, reached the maximum at 0.67 mM, and then decreased (Fig. 6) [60]. As shown in Table 2, the $C^3$–H/$C^2$–H values were in the range of 10.6–14.0, which is characteristic of the radical-mediated oxidations [61]. The independence of the rate on $p_{O_2}$, the bell-shaped dependence of the rate on the concentration of catalyst, and the $C^3$–H/$C^2$–H values strongly suggest that the present oxidation proceeds via a free radical autooxidation mechanism. First, the oxidation is initiated via the one-electron transfer from adamantane to the catalyst to give the reduced form and adamantyl radical species (R·) according to Eq. (1) ($\text{catalyst}_{ox} = V^{5+} + PMo_{12}O_{40}{}^{3-}$, $\text{catalyst}_{red} = V^{4+} + PMo_{12}O_{40}{}^{3-}$ or $V^{5+} + PMo_{12}O_{40}{}^{4-}$).[3] The reduced species then reacts with molecular oxygen to regenerate the oxidized form according to Eq. (2). The radical R· reacts with molecular oxygen to form ROO· [Eq. (3)], which in turn reacts either with adamantane [Eq. (4)] or with a second ROO· species [Eq. (5)].[4] The observed induction period shows that the reaction requires the accumulation of reactive species. A decrease in the induction period with the addition of AIBN or TBHP suggests that R· and hydroperoxide species (ROOH) are the reactive species in the present oxidation. Thus, the induction period would be needed to build up sufficient chain carriers such as R· and ROO· by the reaction among catalyst, adamantane, and molecular oxygen according to Eqs. (1)–(5). The initial formation of R· is a key step in the present oxidation and may take place mainly on the vanadium

$$\text{catalyst}_{ox} + RH \rightarrow \text{catalyst}_{red} + H^+ + R\cdot, \quad (1)$$

$$\text{catalyst}_{red} + H^+ + \tfrac{1}{4}O_2 \rightarrow \text{catalyst}_{ox} + \tfrac{1}{2}H_2O, \quad (2)$$

$$R\cdot + O_2 \rightarrow ROO\cdot, \quad (3)$$

$$ROO\cdot + RH \rightarrow R\cdot + ROOH, \quad (4)$$

$$ROO\cdot + ROO\cdot \rightarrow ROOOOR, \quad (5)$$

species such as $V^VO_2{}^+$, and phosphomolybdate, $PMo_{12}O_{40}{}^{n-}$, enhances the activity. Another important role of the catalyst is likely the decomposition of ROOH species into free radical species.

[3] When $H_4PVMo_{11}O_{40}$ (1.67 mM) in acetic acid was reduced by 200 equivalents of 1,3-dimethyladamantane at 356 K for 4 h under 1 atm of argon, the ESR spectrum of the solution at 4 K showed a signal at $g = 2.005$ in addition to the hyperfine structure of vanadium (see Fig. S4 in the supplementary material). The signal may be assigned to an alkyl radical species.

[4] The reaction of two ROO· species [Eq. (5)] produces very unstable dialkyltetraoxide, ROOOOR, which quickly decomposes into molecular oxygen and two RO· species. Then the RO· species can react with adamantane to form the corresponding alcohol and R· species. In a side recombination reaction, dialkylperoxide ROOR, can be also formed.

## 4. Conclusion

We could develop an adamantane oxidation system with vanadium-substituted polyoxometalates and 1 atm of molecular oxygen without any additives such as reductants and radical initiators. Spectroscopic data show that elimination of the vanadium from the framework of phosphomolybdate Keggin anions occurs to form free vanadium species and $PMo_{12}O_{40}{}^{3-}$ Keggin anions during the reaction. The reaction would be promoted mainly by the vanadium species, and $PMo_{12}O_{40}{}^{n-}$ enhances the activity. The catalyst generates adamantyl radicals by the abstraction of one electron from adamantane.

## Acknowledgments

This work was supported in part by the Core Research for Evolutional Science and Technology (CREST) program of the Japan Science and Technology Agency (JST) and a Grant-in-Aid for Scientific Research from the Ministry of Education, Culture, Sports, Science, and Technology of Japan.

## Supplementary material

The online version of this article contains additional supplementary material.

Please visit DOI:10.1016/j.jcat.2005.04.012.

## References

[1] R.A. Sheldon, J.K. Kochi, Metal Catalyzed Oxidation of Organic Compounds, Academic Press, New York, 1981.
[2] C.L. Hill, in: A.L. Baumstark (Ed.), Advances in Oxygenated Processes, vol. 3, JAI Press, London, 1998, p. 1.
[3] M. Hudlucky, Oxidations in Organic Chemistry, ACS Monograph Series, American Chemical Society, Washington, DC, 1990.
[4] X. Wan, M. Duncan, P. Nass, J.W. Harmon, Anticancer Res. 21 (2001) 2657.
[5] N. Shida, T. Ushiroguchi, K. Asakawa, T. Okino, S. Saito, Y. Funaki, A. Takaragi, K. Tsutsumi, K. Inoue, T. Nakao, J. Photopolym. Sci. Technol. 13 (2000) 601.
[6] N. Matsuzawa, S. Takechi, T. Ohfuji, K. Kuhara, S. Mori, M. Endo, K. Kamon, T. Morisawa, A. Yamaguchi, M. Sasago, Jpn. J. Appl. Phys. 37 (1998) 5781.
[7] H. Stetter, Angew. Chem. 66 (1954) 217.
[8] H. Stetter, M. Schwarz, A. Hirschhorn, Chem. Ber. 92 (1959) 1629.
[9] H. Stetter, E. Rauscher, Chem. Ber. 93 (1960) 1161.
[10] G.W. Smith, H.D. Williams, J. Org. Chem. 7 (1961) 2207.
[11] Y. Ishii, J. Mol. Catal. A 117 (1997) 123.
[12] Y. Ishii, T. Iwasawa, S. Sakaguchi, K. Nakayama, Y. Nishiyama, J. Org. Chem. 61 (1996) 4520.
[13] T. Funabiki, H. Ishida, S. Yoshida, Chem. Lett. (1991) 1819.
[14] I. Yamanaka, K. Nakazaki, T. Akimoto, K. Otsuka, J. Chem. Soc., Perkin Trans. 2 (1996) 2511.
[15] N. Kitajima, M. Ito, H. Fukui, Y. Moro-oka, J. Chem. Soc., Chem. Commun. (1991) 102.
[16] P. Battioni, J.F. Bartoli, P. Leduc, M. Fontecave, D. Mansuy, J. Chem. Soc., Chem. Commun. (1987) 791.
[17] D.H.R. Barton, R.S. Hay-Motherwell, W.B. Motherwell, Tetrahedron Lett. 24 (1983) 1979.
[18] N. Komiya, T. Naota, Y. Oda, S.-I. Murahashi, J. Mol. Catal. A: Chem. 117 (1997) 21.
[19] S.-I. Murahashi, T. Naota, N. Komiya, Tetrahedron Lett. (1995) 8059.
[20] R. Giannandrea, P. Mastrorilli, C.F. Nobile, G.P. Suranna, J. Mol. Catal. 94 (1994) 27.
[21] S.-I. Murahashi, Y. Oda, T. Naota, J. Am. Chem. Soc. 114 (1992) 7913.
[22] K. Yamaguchi, N. Mizuno, New. J. Chem. 26 (2002) 972.
[23] R. Neumann, M. Dahan, J. Am. Chem. Soc. 120 (1998) 11969.
[24] N. Mizuno, M. Tateishi, T. Hirose, M. Iwamoto, Chem. Lett. (1993) 2137.
[25] M.M.T. Khan, D. Chatterjee, S. Kumar, A.P. Rao, N.H. Khan, J. Mol. Catal. 75 (1992) L49.
[26] I.V. Kozhevnikov, Catalysis by Polyoxometalates, Wiley, Chichester, England, 2000.
[27] R. Neumann, Prog. Inorg. Chem. 47 (1998) 317.
[28] N. Mizuno, M. Misono, Chem. Rev. 98 (1998) 199.
[29] T. Okuhara, N. Mizuno, M. Misono, Adv. Catal. 41 (1996) 113.
[30] C.L. Hill, C.M. Prosser-McCartha, Coord. Chem. Rev. 143 (1995) 407.
[31] M.T. Pope, A. Müller, Angew. Chem. Int. Ed. Engl. 30 (1991) 34.
[32] K. Kamata, K. Yonehara, Y. Sumida, K. Yamaguchi, S. Hikichi, N. Mizuno, Science 300 (2003) 964.
[33] W. Adam, P.L. Alsters, R. Neumann, C.R. Saha-Möller, D. Sloboda-Rozner, R. Zhang, J. Org. Chem. 68 (2003) 1721.
[34] D. Sloboda-Rozner, P.L. Alsters, R. Neumann, J. Am. Chem. Soc. 125 (2003) 5280.
[35] N.M. Okun, T.M. Anderson, C.L. Hill, J. Am. Chem. Soc. 125 (2003) 3194.
[36] H. Weiner, A. Trovarelli, R.G. Finke, J. Mol. Catal. A 191 (2003) 253.
[37] A.M. Khenkin, R. Neumann, Adv. Synth. Catal. 344 (2002) 1017.
[38] S. Ellis, I.V. Kozhevnikov, J. Mol. Catal. A 187 (2002) 227.
[39] R. Ben-Daniel, L. Weiner, R. Neumann, J. Am. Chem. Soc. 124 (2002) 8788.
[40] H. Tsuji, Y. Koyasu, J. Am. Chem. Soc. 124 (2002) 5608.
[41] J.T. Rhule, W.A. Neiwert, K.I. Hardcastle, B.T. Do, C.L. Hill, J. Am. Chem. Soc. 123 (2001) 12101.
[42] I.A. Weinstock, E.M.G. Barbuzzl, M.W. Wemple, J.J. Cowan, R.S. Reiner, D.M. Sonnen, R.A. Heintz, J.S. Bond, C.L. Hill, Nature 414 (2001) 191.
[43] Y. Nishiyama, Y. Nakagawa, N. Mizuno, Angew. Chem. Int. Ed. 40 (2001) 3639.
[44] T. Hayashi, A. Kishida, N. Mizuno, Chem. Commun. (2000) 381.
[45] T. Yokota, M. Tani, S. Sakaguchi, Y. Ishii, J. Am. Chem. Soc. 125 (2003) 1476.
[46] M. Vennat, P. Herson, J.-M. Brégeault, G.B. Shul'pin, Eur. J. Inorg. Chem. (2003) 908.
[47] R. Ben-Daniel, R. Neumann, Angew. Chem. Int. Ed. 42 (2003) 92.
[48] T. Yokota, S. Sakaguchi, Y. Ishii, Adv. Syhth. Catal. 344 (2002) 849.
[49] A.M. Khenkin, L. Weiner, Y. Wang, R. Neumann, J. Am. Chem. Soc. 123 (2001) 8531.
[50] C.P. Stewart, A.L. Porte, J. Chem. Soc., Dalton Trans. (1972) 1661.
[51] D.D. Perrin, in: W.L.F. Armarego (Ed.), Purification of Laboratory Chemicals, third ed., Pergamon Press, Oxford, UK, 1988.
[52] G.A. Tsigdinos, C.J. Hallada, Inorg. Chem. 7 (1968) 437.
[53] R. Bayer, C. Marchal, F.X. Liu, A. Tézé, G. Hervé, J. Mol. Catal. A: Chem. 110 (1996) 65.
[54] C. Marchal-Roch, N. Laronze, N. Guillou, A. Tézé, G. Hervé, Appl. Catal. A 199 (2000) 33.
[55] R. Neumann, M. Levin, J. Am. Chem. Soc. 114 (1992) 7278.
[56] L. Pettersson, I. Andersson, A. Selling, J.H. Grate, Inorg. Chem. 33 (1994) 982.

[57] N. Mizuno, H. Yahiro, J. Phys. Chem. B 102 (1998) 437.
[58] J.J. Altenau, M.T. Pope, R.A. Prados, H. So, Inorg. Chem. 14 (1975) 417.
[59] C. Slebodnick, V.L. Pecoraro, Inorg. Chim. Acta 283 (1998) 37.
[60] A similar decrease in the rate with the increase in the catalyst concentration was reported for the alkane oxidation system with $O_2$/aldehydes involving radical species, and it is suggested that the catalyst might act as an inhibitor at higher catalyst concentration. See (a) A.M. Khenkin, A. Rosenberger, R. Neumann, J. Catal. 182 (1999) 82;
(b) O.A. Kholdeeva, V.A. Grigoreiv, G.M. Maksimov, M.A. Fedotov, A.V. Golovin, K.I. Zamaraev, J. Mol. Catal. 114 (1996) 123.
[61] M. Bonchio, G. Scorrano, P. Toniolo, A. Proust, V. Artero, V. Conte, Adv. Synth. Catal. 344 (2002) 841.